PERGAMON

Available online at www.sciencedirect.com

SCIENCE DIRECT®

Scripta Materialia 49 (2003) 953–959

Scripta MATERIALIA

www.actamat-journals.com

Spontaneous formation of patterns on sputtered surfaces

Eric Chason [a,*], Michael J. Aziz [b]

[a] *Division of Engineering, Brown University, Box D, Providence, RI 02912, USA*
[b] *Division of Engineering and Applied Sciences, Harvard University, Cambridge, MA 02138, USA*

Accepted 23 July 2003

Abstract

Sputtering by collimated low energy ion beams can spontaneously create periodic structures on many surfaces. The pattern results from the balance between roughening by atom removal and smoothing, typically by surface diffusion. Experiments on a number of surfaces are considered in terms of linear and non-linear models of surface evolution.

Keywords: Self-organization and patterning; Surface structure; Ion beam processing; Sputtering

1. Introduction

Controlling and manipulating surface morphology on the nano- and micro-scale is important for many present and future technological applications. As length scales decrease below the range easily accessible by lithographic patterning, there is great interest in developing processes to form surface structures spontaneously. In these systems, the pattern is produced by the interaction of basic physical processes to generate a periodic structure instead of imposing one via a template or serial writing. One such method to spontaneously create patterns on the surfaces of many materials is low energy ion bombardment or sputtering. Even though the flux of the ion beam is uniform, periodic structures (called sputter ripples) are observed to develop as the initially flat surface is sputtered.

Here we review the fundamental physical mechanisms that lead to sputter ripple formation. In the spirit of this viewpoint series, we discuss these in terms of the concept of a driven process, where the incident ion beam drives the system away from the equilibrium flat surface morphology. We also review some of the phenomenology to point out the differences between materials classes and the significance this has for our understanding of surface transport in different materials.

Ion bombardment has been used for many years as a way to create non-equilibrium conditions for the study of materials processes (several examples are given in Ref. [1]). High energy ions create Frenkel pairs deep within a crystalline solid which typically have high mobilities, thereby accelerating structural re-organization. Low energy ions, in contrast, deposit their energy barely below the surface of solids and therefore can cause the

* Corresponding author. Tel.: +1-401-8632317; fax: +1-401-8637677.
E-mail address: eric_chason@brown.edu (E. Chason).

1359-6462/$ - see front matter © 2003 Acta Materialia Inc. Published by Elsevier Ltd. All rights reserved.
doi:10.1016/S1359-6462(03)00474-3

sputter-removal of surface atoms. Because the atom is most likely to be sputtered where the energy deposited by the ion is closest to the surface, the sputter yield can depend on the local surface morphology. This interaction between sputter yield and surface structure leads to instabilities and the spontaneous pattern formation.

2. Ion-induced surface patterns

Sputter ripples have been seen in a wide range of materials: semiconductors, insulators, amorphous oxides and metals (see articles cited in Refs. [2,3]). Initially, the ripples were seen in SEM images only after large amounts of material had been removed. More recently the use of STM and AFM have provided much more detailed measurements of the ripple morphology. X-ray [4,5] and light [6] scattering have also been used to study the kinetics of the ripple formation.

An AFM image of a sputter ripple is shown in Fig. 1 for a Si(0 0 1) surface bombarded with 750 Ar^+ ions at 600 °C [7]. The pattern was produced by a collimated ion beam with uniform flux of approximately 0.7 mA/cm^2. The angle of incidence of the ion relative to the surface is 55° from the surface normal. The beam was not rastered across the surface in order to produce the pattern. The wavelength of the resulting ripple is approximately

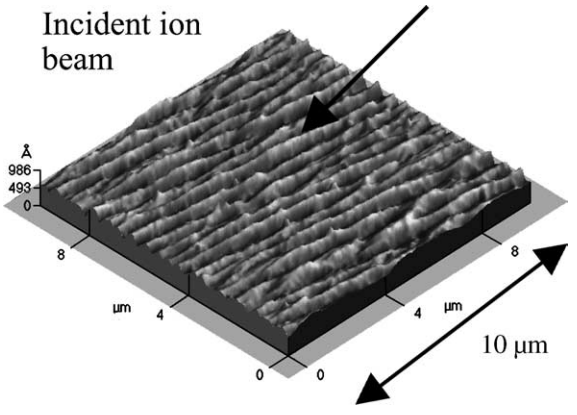

Fig. 1. AFM image of a sputter ripple produced on a Si(0 0 1) surface. The pattern was produced by bombardment with 750 eV Ar^+ ions at 600 °C and a flux of 0.7 mA/cm^2. From Cuenat and Aziz [7].

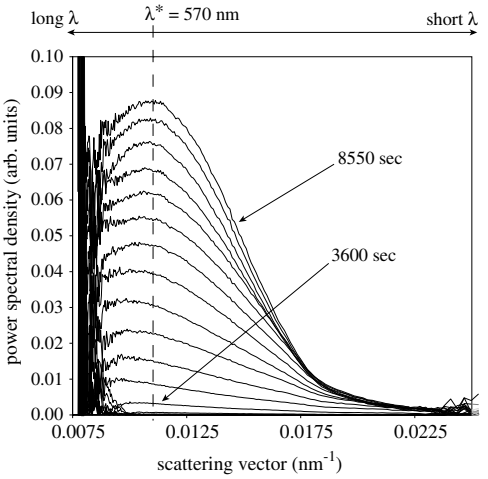

Fig. 2. Power spectral density (PSD) of Si(0 0 1) surface during various stages of ripple formation. The sputtering conditions are identical to those described in Fig. 1. The displayed spectra are separated by equal intervals of sputter time. The PSD's were obtained using an in situ light scattering measurement technique. From Erlebacher et al. [6].

520 nm. The structure is fairly well organized and is found over large areas of the surface.

To study the evolution of the sputter ripple, light scattering [6] has also been used to measure the power spectral density (PSD) of the surface morphology during ripple formation. The surface PSD for a Si(0 0 1) surface (similar to that shown in Fig. 1) is shown in Fig. 2 [6]. The data have been normalized to the scattering from an initially flat surface. As the surface is sputtered, the PSD develops a peak corresponding to the formation of a periodic structure on the surface. Note that for the Si surface shown in the figure, the predominant spatial period of the structure does not change significantly during the sputtering over the range of fluences measured. The dependence of the ripple periodicity on ion and material parameters is discussed further below, along with comparisons between materials systems.

3. Theory of ripple formation

For the purpose of this viewpoint set, the most significant feature of the ripple formation is that the pattern occurs spontaneously with no imposed

template. The first explanation of the phenomenon, proposed by Bradley and Harper [8] (BH), was a linear instability theory. In this approach, ion bombardment acts as a driving force to roughen the surface and surface diffusion acts to restore the surface to its flat equilibrium state. The competition between the two processes results in the selection of a preferred wavelength that grows faster than any other. Though the theory is valid only for small-amplitude structures, it has been surprisingly successful as a basic guide to ripple formation. Several modifications to the theory have been proposed [2,3,9] that enable it to be extended to the non-linear regime, some of which are discussed in later sections.

The rate of surface roughening is based on a mechanism proposed by Sigmund [10] that describes the sputter process in terms of the energy deposited by the ion as it slows down through a series of collisions in the solid as it comes to rest at an average range of a_0. The collision cross section actually increases as the ion slows down, resulting in greater energy deposition below the surface than at the surface. Considering the statistical result of a large number of ion collisions, Sigmund proposed that the energy is deposited in 3-D ellipsoidal Gaussian contours around the end of the ion track. If the ion range is short enough then there is sufficient energy deposited near the surface to cause sputtering of an atom. Bradley and Harper extended this theory to show how the surface can become unstable to small-amplitude periodic disturbances. If the interaction of the surface morphology with the energy deposition is considered, the local sputter yield is proportional to the curvature of the surface. The surface morphology then evolves according to

$$\frac{\partial h}{\partial t} = S_x \frac{\partial^2 h}{\partial x^2} + S_y \frac{\partial^2 h}{\partial y^2}, \tag{1}$$

where h is the height of the surface relative to the average height. x is defined as the spatial coordinate parallel to the projected direction of the ion beam on the plane of average surface orientation and y is the coordinate within this plane perpendicular to x. S_x and S_y are parameters calculated by BH that depend on the ion beam, the angle of incidence and the material. S_y is negative for all angles of incidence and S_x is negative for a range of angles.

Balanced against the roughening caused by the ion beam, there is mass transport induced by a driving force to smoothen the surface in order to reduce surface energy. Using a continuum model of the surface (as developed by Herring [11] and Mullins [12]), the chemical potential of atoms at the surface is proportional to the curvature. Variations in the surface morphology create a gradient in the curvature, driving mass transport away from convex regions of the solid towards concave. If the mass transport pathway is surface diffusion, this effect changes the height of the surface according to the form

$$\frac{\partial h}{\partial t} = -B\nabla^2\nabla^2 h, \tag{2}$$

where $B = D_s\gamma C/n^2 k_B T$, D_s is the surface diffusivity, γ is the surface free energy per unit area, C is the concentration of mobile species, and n is the areal concentration of atomic sites. Although all sputter-rippling models of which we are aware use some form of this classical capillary term, there is evidence that the effects of surface steps on both the thermodynamics [13] and the kinetics [14] of the smoothing process, which are not embodied in Eq. (2), are important—at least on unirradiated surfaces.

The evolution of the surface during ion bombardment is the result of both these processes acting simultaneously. Since both Eqs. (1) and (2) are linear, we can rewrite the equations to express the decoupled evolution of individual Fourier components of the PSD. If we define h_q as the Fourier transform of the surface height and $\mathbf{q}$ as the surface wave vector of interest,

$$\frac{\mathrm{d}h_q}{\mathrm{d}t} = -(S_x q_x^2 + S_y q_y^2)h_q - B(q_x^2 + q_y^2)^2 h_q. \tag{3}$$

The solution is of the form $h_q(0)\exp(R_q t)$ where $h_q(0)$ is the initial amplitude of the Fourier component and R_q is an amplification factor with the form:

$$R_q = -(S_x q_x^2 + S_y q_y^2) - B(q_x^2 + q_y^2)^2. \tag{4}$$

For values of q_x and q_y such that R_q is positive, the amplitude of the Fourier component increases

with time. For these wave vectors, roughening overwhelms smoothing. For wave vectors with negative R_q, the smoothing term is dominant and the amplitude decays. R_q has a maximum at the value $q^* = (S_{\max}/2B)^{1/2}$ where $S_{\max}$ is the larger of the two values $-S_x$ and $-S_y$. As the amplitude at this wavenumber grows faster than all others, the result is a surface that has a preferred periodicity with wavenumber q^*. The wave vector will be aligned along the x-direction if $-S_x > -S_y$, and along the y-direction if $-S_y > -S_x$. The values of S_x and S_y depend on the angle of incidence so that the ripple orientation can rotate from along the x-axis to along the y-axis by changing the angle of the ion beam relative to the surface. The predicted change in orientation of the ripples with angle has been seen experimentally and is one of the most compelling aspects of the model.

Although many of the basic features of ripple formation are explained by this model, the picture is too simple to explain the full range of observations. Several groups have suggested modifications to the basic theory to make it more in agreement with experiment. Cuerno and Barabasi [9] proposed non-linear terms that are consistent with the observed saturation of the ripple at large amplitude. The non-linear equation is

$$\frac{\partial h}{\partial t} = K\frac{\partial h}{\partial x} + S_x\frac{\partial^2 h}{\partial x^2} + S_y\frac{\partial^2 h}{\partial y^2} + \eta_x\left(\frac{\partial h}{\partial x}\right)^2 + \eta_y\left(\frac{\partial h}{\partial y}\right)^2 - B\nabla^2\nabla^2 h + \Gamma(x,y,t), \quad (5)$$

where K, η_x and η_y are coefficients calculated by Cuerno and Barabasi, and $\Gamma(x,y,t)$ is a noise term.

Makeev and Barabasi [15] carried out an expansion of the interaction of the ion with the surface to higher order in the derivatives of $h(x,y)$ and showed that there are fourth-order terms, similar to the diffusional term in Eq. (2), that act to smooth the surface even in the absence of diffusion. Thus there can be a preferred wave vector and ripple structure produced on the surface at low temperature even in the absence of thermally-activated surface diffusion. Effects of surface crystallography and diffusion on the stepped surfaces may also be included and will be discussed below in reference to metallic systems.

4. Dependence of ripple formation on processing parameters

With the insight into ripple formation provided by the BH theory and its modifications, we can consider the morphological response of the system to the driving force of ion bombardment and the restoring force of surface diffusion. Makeev et al. [2] have utilized the non-linear theory to develop "phase diagrams" for the regions of parameter space over which ripples with various characteristics form. With an equation as complicated as (5), these phase diagrams are multidimensional and only rudimentarily explored both theoretically and experimentally. Fig. 3 shows a section of this multidimensional phase diagram appropriate for Eq. (5) and discussed in Ref. [2]. This type of phase diagram is different from those typically seen in a Martin–Bellon [1] theory of driven systems. The independent variables are not kinetic parameters but instead the ratio of the ion range to the width of the collision cascade, a_σ, and the angle of incidence θ, defined relative to the surface normal. The regions are determined by the signs of the parameters $(S_x, S_y, \eta_x, \eta_y)$ which depend on a_σ and θ to select a most-rapidly-amplifying morphology. Kinetic parameters such as surface diffusion and flux are important in determining the ripple wavelength and the rate at which it grows, but the "qualita-

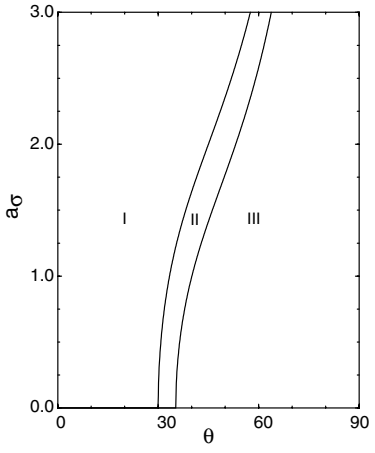

Fig. 3. Phase diagram of the dependence of ripple formation on a_σ (the ratio of the ion's range to its width) and angle of incidence. From Makeev et al. [2].

tive" behavior of which type of ripples form and whether they are stable are determined by geometric effects due to the incidence angle and the collision cascade.

Region I in the figure corresponds to the case where S_x, S_y, η_x and η_y are all negative. At short times, the theory predicts ripple formation oriented along the x- or y-direction depending on the relative magnitude of S_x and S_y as described above for the linear theory. At long times, the amplitude grows to a point that the non-linear terms take over, the ripple structure disappears and the surface undergoes kinetic roughening. In region II, S_x and S_y are negative and η_x and η_y have opposite signs. Studies by Park et al. [16] indicate that ripples form in the early stages followed by roughening. At longer times, however, a new ripple structure forms in which the ripples are rotated relative to the x-direction. In region III, $S_x > 0$ and $S_y < 0$. At short times, ripples are formed with wave vector oriented along the y-direction. The long-time behavior is complicated but analysis suggests that a rotated ripple morphology will develop similar to region II.

The non-linear equation predicts that in some regimes the ripples should grow exponentially in the early stages and then transition to roughening behavior. As discussed above, light scattering measurements of sputtered Si(0 0 1) surfaces [6] have been used to study the evolution of the ripple amplitude in real time. The data in Fig. 4 show measurements [17] of the ripple amplitude made at various ripple wavelengths and surface temperatures as indicated in the figure. In the very early stages, the peak intensity seems to grow exponentially. At higher fluences and peak amplitudes, the rate of growth decreases dramatically. By scaling the sputtering time by $S_{\max}^2/4B$ and the amplitude by $(S_{\max}/2B)^{1/2}$, the data from multiple sputtering runs at different temperatures and fluxes collapse to similar behavior for a wide range of wavelengths and temperatures. Measurements of surface roughness on sputtered graphite demonstrate a similar transition from early exponential growth, in this case to kinetic roughening at a later stage [18].

In the regions where ripples form, the ripple wavelength λ is predicted to depend on the processing parameters f, θ, and T in the following way:

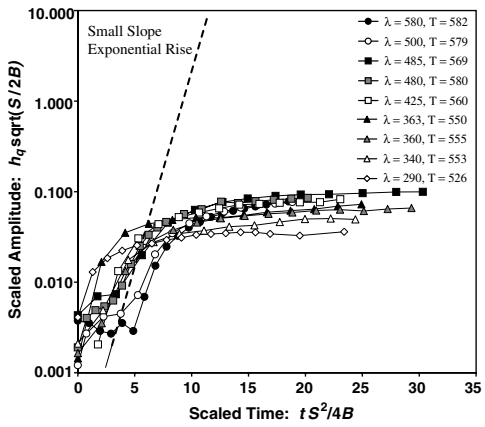

Fig. 4. Non-linear evolution of ripple amplitude on Si surfaces measured by light scattering. From Erlebacher et al. [17].

$$\lambda = \frac{2\pi}{q^*} = 2\pi\left(\frac{2B}{S_{\max}}\right)^{1/2} \propto \left(\frac{D_s(T)C(f,T)}{S_{\max}(f,\theta)T}\right)^{1/2}, \tag{6}$$

where f is the ion flux. The diffusivity is temperature dependent and the concentration of mobile species may depend on the temperature and the flux. S depends linearly on f and in a more complex way on the angle of incidence. This prediction of the unstable wavelength from the linear theory is only valid for the early stages of ripple formation, but in many systems (particularly semiconductors and amorphous materials) the observed wavelength does not change even with extended sputtering time.

Although based on a simple theory, this dependence of the wavelength on sputtering parameters is consistent with a number of experiments. Erlebacher et al. [6] found that the measured wavelength on Si had an Arrhenius temperature dependence over the temperature range studied (470–580 °C) with an activation energy of 1.2 eV. This is consistent with the 1.1 eV migration energy measured independently [19] for dimers on the surface and suggests that the concentration of the mobile surface species does not depend on the temperature. The mobile species are produced and annihilated

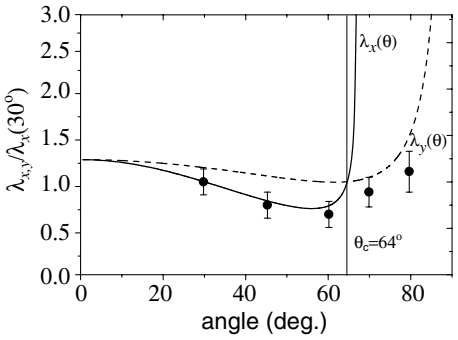

Fig. 5. Observation of ripple rotation transition with increasing angle, from Habenicht et al. [21]. Curves show predicted wavelength for wave vectors along x and y vs. angle.

athermally and not by a thermally-activated process such as detachment from step edges. In addition, the flux dependence is $\lambda \propto f^{-1/2}$. This behavior indicates, through Eq. (6), that the mobile defect concentration is independent of ion flux and suggests that the predominant annihilation mechanism of mobile defects is direct ion impingement rather than annihilation at sinks such as surface steps [6]. In other systems [20], however, the wavelength has been found to be independent of flux, so that the defect concentration may also be controlled by the annihilation of defects at sinks.

Habenicht et al. [21] have measured the angular dependence of the parameters S_x and S_y by measuring the ripple wavelength as a function of the angle of incidence on graphite surfaces. As shown in Fig. 5, they observe a rotation of the ripple wave vector from along the x-direction to along the y-direction, consistent with the predictions of the Bradley–Harper mechanism.

5. Ripple formation on metals: effects of surface crystallography

The theory as discussed above does not include any effects of crystallographic orientation. In this form, it is sufficient to explain many measurements on semiconductor and amorphous materials, in which the direction of the surface pattern is observed to depend on the angle of the ion beam relative to the surface normal but not on the direction of the beam relative to the surface crystallography. However, experiments on many metals [4,22,23] demonstrate that the surface crystallography can play an important role in the pattern formation. Measurements by Rusponi et al. on Cu(1 1 0) surfaces [23] showed that the pattern rotated when the crystal surface was rotated azimuthally while keeping the angle of incidence of the ion fixed at 45° relative to the surface normal. These experiments indicate the importance of surface crystallography and azimuthal anisotropies on pattern formation.

To account for these effects, Rusponi et al. proposed a modification to the theory that effectively includes crystal anisotropy in certain of the parameters in Eq. (5). The physical motivation is the effect of an Ehrlich–Schwoebel (ES) barrier which impedes the diffusion of adatoms over downward surface steps and thereby drives a net uphill surface current. Because this term is diffusive in origin, it leads to pattern formation during atom deposition as well as ion bombardment. When the predominant effect of the ion beam is the creation of mobile species and the interaction geometry of the incoming particle with the surface is unimportant, the resulting pattern is not dependent on the direction of the incoming ions. Unlike in BH theory, this diffusive term does not predict a fixed ripple wavelength. Experiments on metal surfaces show that the ripple wavelength increases with the duration of the sputtering as a power law with an exponent of +0.26 for the measurements on Cu(1 1 0) surfaces [24]. The absence of these crystallographic effects in semiconductor systems may be due either to lower ES barriers or processing conditions in which the diffusive terms are not significant.

Behavior more similar to the BH theory has also been observed in metals. In the experiments on Cu(1 1 0) surfaces discussed above, when the incidence angle was increased to 70°, the pattern became oriented along the ion beam direction. Valbusa et al. [3] describe this as a transition between "diffusive regime" where anisotropies in surface transport dominate and the "erosive regime" where the pattern formation is dominated by ion–surface interactions. Recently, ripples have been created on Cu(1 0 0) surfaces that have a constant wavelength, so it may be possible to have

both fixed wavelength and power-law regimes depending on the kinetic parameters used [25].

Finally, we note that not all measurements of ion beam patterning have been fully explained within this framework. Facsko et al. [26] have observed nanoscale patterning on GaSb surfaces during normal incidence irradiation. The resulting quantum dots have smaller length scales and higher aspect ratios than have been observed in other systems and may point to other ion-induced pattern forming mechanisms not considered here. Additionally, we mention the availability of other control parameters, such as continuous sample rotation [27] or rastering parameters in the formation of sputter ripples using a focused ion beam (FIB) [7,28].

6. Conclusion

A low energy ion-irradiated solid surface may be thought of as a "driven system". The balance between roughening due to sputtering and various smoothing mechanisms can lead to a wide range of morphologies. The response of the system to these driving forces can lead to the spontaneous formation of self-organized ripples, dots, or pits on these surfaces. However, our current understanding is that the complicated non-linear nature of the interaction between the surface and the sputtering process does not lead to simple steady-state behavior as in other driven systems. Systematic experimental studies of different materials systems and sputtering conditions are just beginning to unravel the wide range of behavior that can be found.

Acknowledgements

The authors gratefully acknowledge the support of US Department of Energy under contract # DE-FG02-01ER45947 (Harvard) and DE-FG02-01ER45913 (Brown). The authors also thank Jonah Erlebacher, Wai Lun Chan, Alexandre Cuenat, Jerrold Floro and Michael Sinclair for their helpful contributions as collaborators to the work reviewed here.

References

[1] Martin G, Bellon P. In: Ehrenreich H, Spaepen F, editors. Solid state physics, vol. 50. San Diego: Academic Press; 1997. p. 189–332.
[2] Makeev MA, Cuerno R, Barabasi A-L. Nucl Instrum Meth B 2002;197:185.
[3] Valbusa U, Boragno C, Buatier de Mongeot F. J Phys: Condens Matter 2002;14:8153.
[4] Murty MVR, Curcic T, Judy A, Cooper BH, Woll AR, Brock JD, et al. Phys Rev Lett 1998;80:4713.
[5] Mayer TM, Chason E, Howard AJ. J Appl Phys 1994;76:1633.
[6] Erlebacher J, Aziz MJ, Chason E, Sinclair MB, Floro JA. Phys Rev Lett 1999;82:2330.
[7] Cuenat A, Aziz MJ. In: MRS Symp Proc, vol. 696. 2002. p. N2.8.
[8] Bradley RM, Harper JM. J Vac Sci Technol A 1988;6:2390.
[9] Cuerno R, Barabasi A-L. Phys Rev Lett 1995;74:4746.
[10] Sigmund P. J Mater Sci 1973;8:1545;
Sigmund P. Phys Rev 1969;184:383.
[11] Herring C. In: Kingston WE, editor. Physics of powder metallurgy. New York: McGraw-Hill; 1951;
Herring C. J Appl Phys 1950;21:301.
[12] Mullins WW. J Appl Phys 1959;30:77.
[13] Jeong H-C, Williams ED. Steps on surfaces: experiment and theory. Surf Sci Rep 1999;34:171–294.
[14] Erlebacher JD, Aziz MJ, Chason E, Sinclair MB, Floro JA. Phys Rev Lett 2000;84:5800;
Israeli N, Kandel D. Phys Rev Lett 2002;88:169601 (comment);
Erlebacher JD, Aziz MJ, Chason E, Sinclair MB, Floro JS. Phys Rev Lett 2002;88:169602 (reply).
[15] Makeev MA, Barbasi A-L. Appl Phys Lett 1997;71:2800.
[16] Park S, Kahng B, Jeong H, Barabasi A-L. Phys Rev Lett 1999;83:3486.
[17] Erlebacher JD, Aziz MJ, Chason E, Sinclair MB, Floro JA. J Vac Sci Technol A 2000;18:115.
[18] Habenicht S. Phys Rev B 2001;63:125419.
[19] Swartzentruber BS. Phys Rev Lett 1996;76:459–62;
Krueger M, Borovsky B, Ganz E. Surf Sci 1997;385:146–54.
[20] Vajo JJ, Doty RE, Cirlin E-H. J Vac Sci Technol A 1996;14:2709.
[21] Habenicht S, Bolse W, Lieb KP, Reimann K, Geyer U. Phys Rev B 1999;60:R2200.
[22] Michely T, Comsa G. Nucl Instrum Meth B 1993;82:207.
[23] Rusponi S, Constantini G, Boragno C, Valbusa U. Phys Rev Lett 1998;81:2735.
[24] Rusponi S, Constantini G, Boragno C, Valbusa U. Phys Rev Lett 1998;81:4184.
[25] van Dijken S, de Bruin D, Poelsema B. Phys Rev Lett 2001;86:4608;
Chan WL, Chason E. Unpublished.
[26] Facsko S, Dekorsy T, Koerdt C, Trappe C, Kurz H, Vogt A, et al. Science 1999;285:1551.
[27] Frost F. Appl Phys A 2002;74:131–3.
[28] Habenicht S, Lieb KP, Koch J, Wieck AD. Phys Rev B 2002;65:115327-1.